Electronic Supplementary Information

N,S-Codoped Hierarchical Porous Carbon Spheres Embedded with Cobalt Nanoparticles as Efficient Bifunctional Oxygen Electrocatalysts for Rechargeable Zinc-Air Batteries

Xiaojing Zhu[a], Jiale Dai[a], Ligui Li[a, b, c,*], Zexing Wu[d], Shaowei Chen[a, e, *]

[a]New Energy Research Institute, School of Environment and Energy, South China University of Technology, Guangzhou Higher Education Mega Centre, Guangzhou, 510006, China.

E-mail: esguili@scut.edu.cn.

[b.] Key Lab of Pollution Control and Ecosystem Restoration in Industry Clusters, Ministry of Education, South China University of Technology, Guangzhou 510641, China.

[c.]State Key Laboratory of Polymer Physics and Chemistry, Changchun Institute of Applied Chemistry, Chinese Academy of Sciences, Changchun 130022, China.

[d.]State Key Laboratory Base of Eco-chemical Engineering, College of Chemistry and Molecular Engineering, Qingdao University of Science & Technology, 53 Zhengzhou Road, 266042, Qingdao, China.

[e.]Department of Chemistry and Biochemistry, University of California, 1156 High street, Santa Cruz, California 95064, USA.

E-mail: shaowei@ucsc.edu.

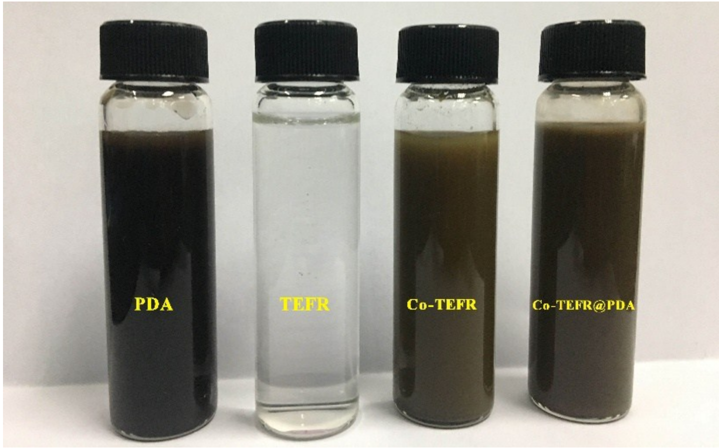

Figure S1. Photographs of different precursor samples.

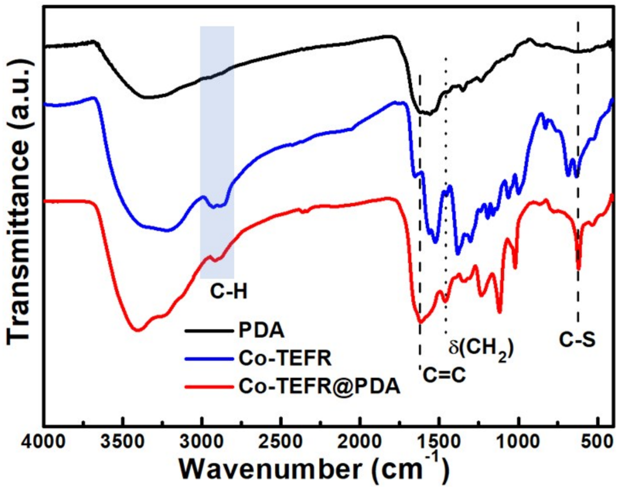

Figure S2. FTIR spectra of various precursor samples.

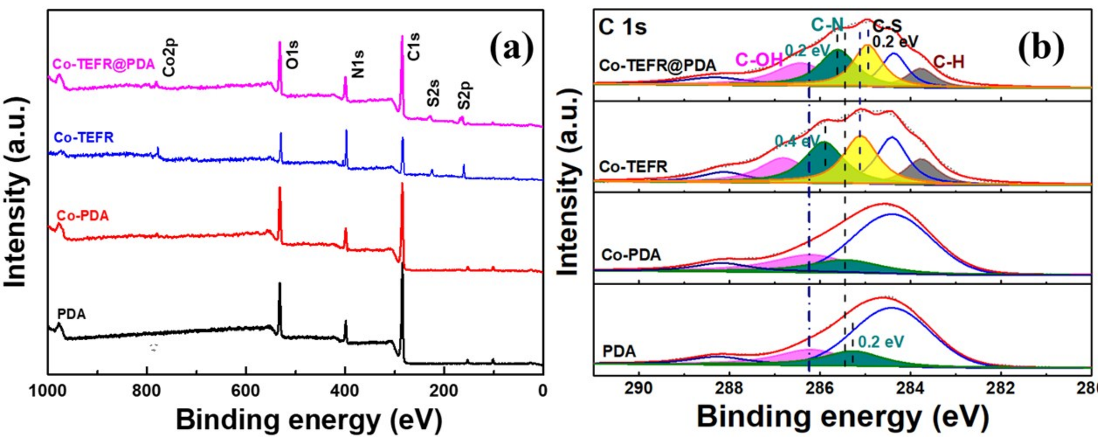

Figure S3. (a) XPS survey spectra and (b) high-resolution C 1s XPS spectra of different precursor samples.

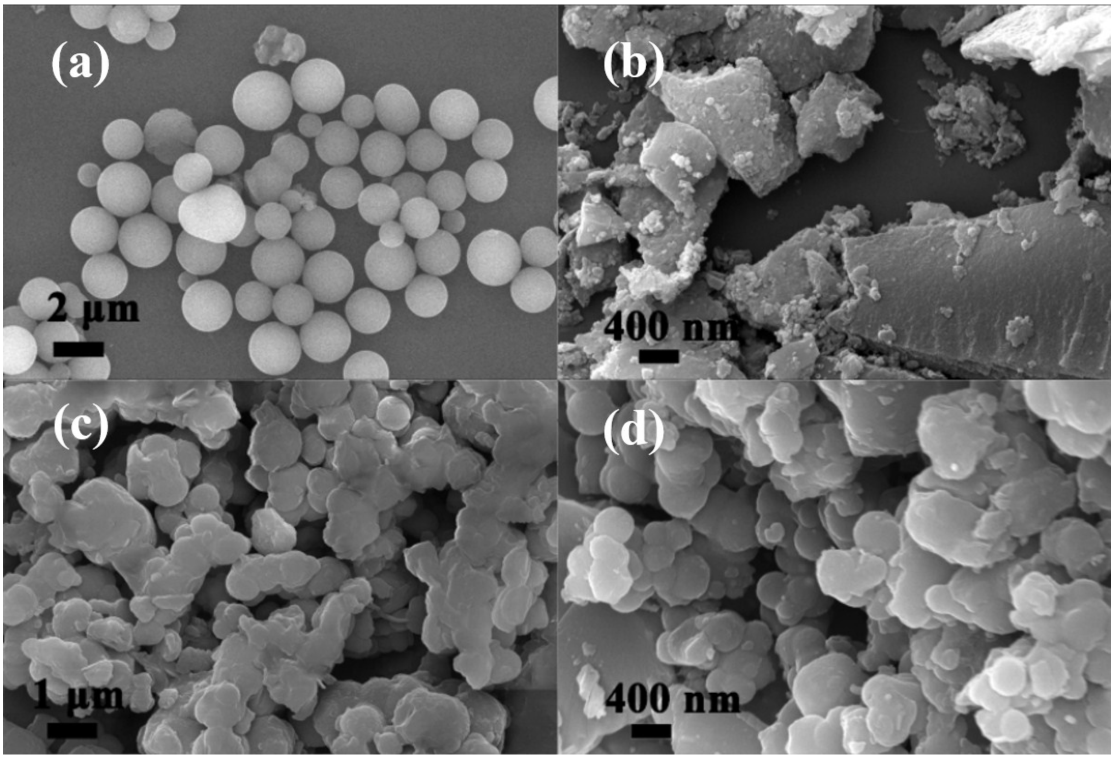

Figure S4. SEM images of (a) precursor Co-TEFR, and (b) the corresponding Co@NSC derived from the carbonization of Co-TEFR, (c) Co-PDA precursor, and (d) the corresponding Co@NC derived from the carbonization of Co-PDA.

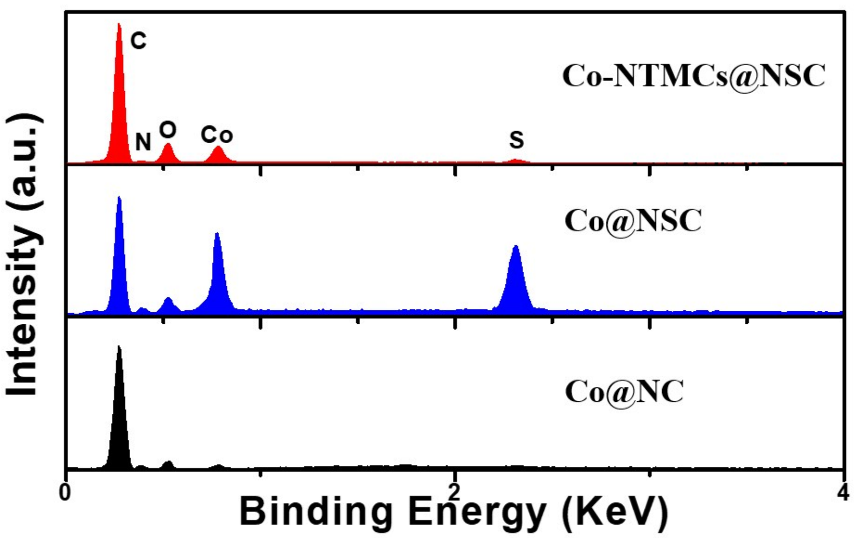

Figure S5. EDS spectra of Co-NTMCs@NSC, Co @NSC and Co@NC.

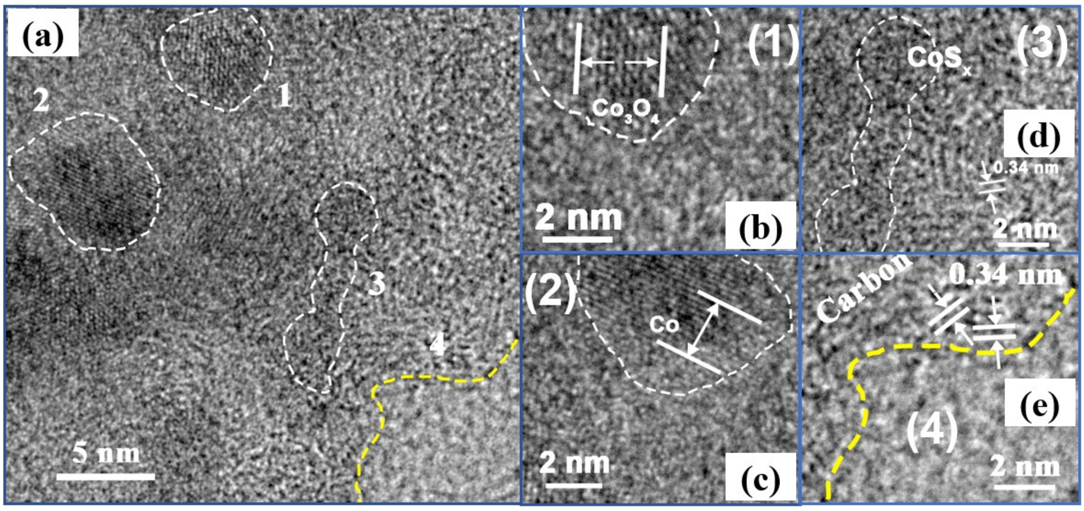

Figure S6. (a) The HR-TEM images of Co-NTMCs@NSC; (b, c, d, e) The enlarged images of the selected region in panel a.

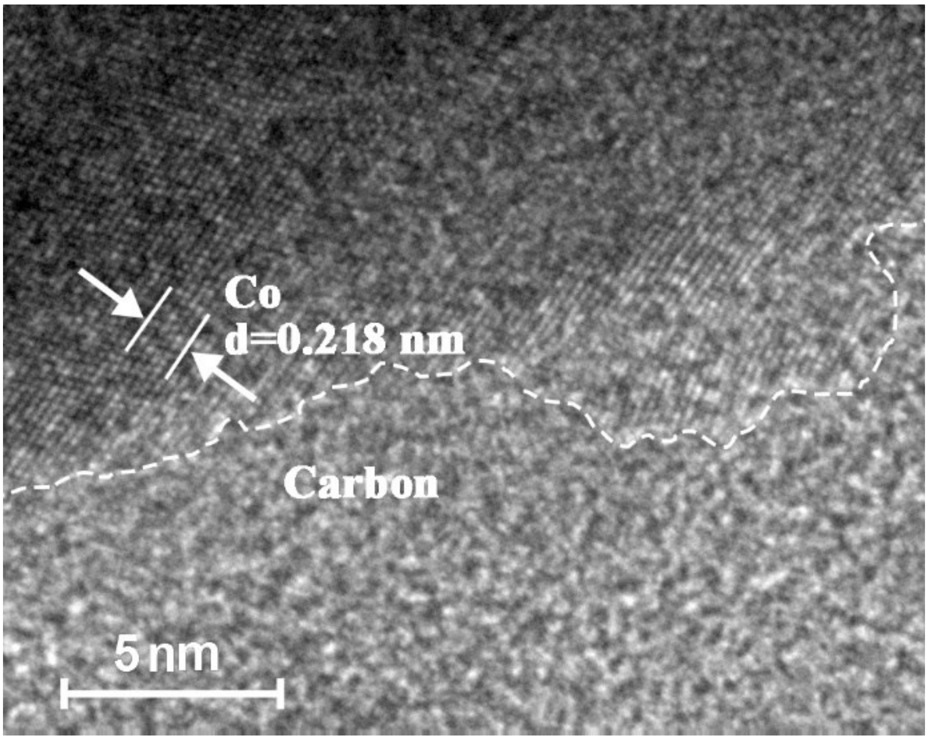

Figure S7. A HR-TEM image of Co-NTMCs@NSC to illustrate the interface between metallic Co and N, S-doped carbon matrix.

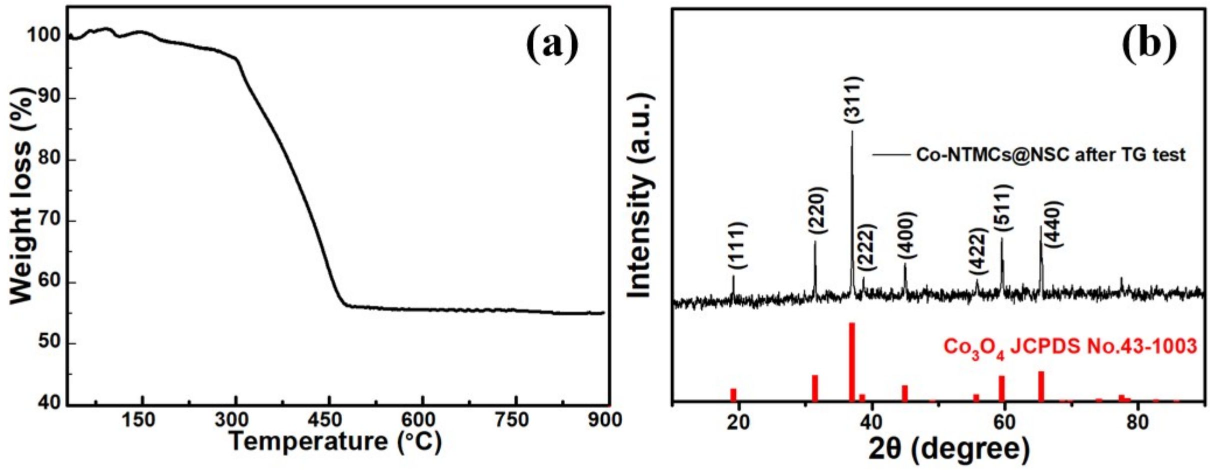

Figure S8. (a) TGA curve of Co-NTMCs@NSC and (b) XRD patterns of the Co-NTMCs@NSC sample after TG test.

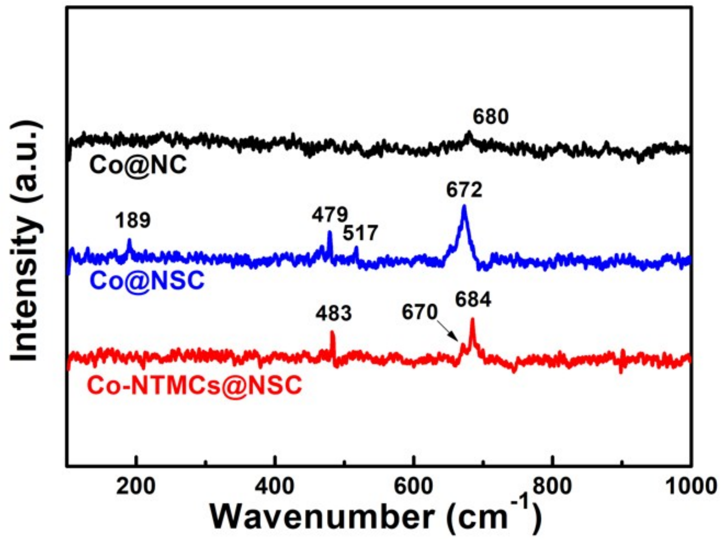

Figure S9. Raman spectra at low wavenumber region of 100−1000 cm^{-1} for Co@NC, Co@NSC and the typical sample Co-NTMCs@NSC.

As shown in Figure S9, the weak peak at 680 cm^{-1} observed in Co@NC is attributed to the vibration of Co-O bond in CoO_x nanoparticles that probably due to the partial oxidation of metallic Co [R1]. Besides, the spectrum for Co@NSC displays typical Raman peaks at 672, 517, 479 and 189 cm^{-1}, which are assigned to vibration of Co-S bond in Co_4S_3 particles. As for Co-NTMCs@NSC, the peaks at 684 and 483 cm^{-1} are assigned to the Co-O vibration, while the one at 670 cm^{-1} is ascribed to the vibration of Co-S bond, indicating the coexistence of CoS_x and Co_3O_4 species in Co-NTMCs@NSC.

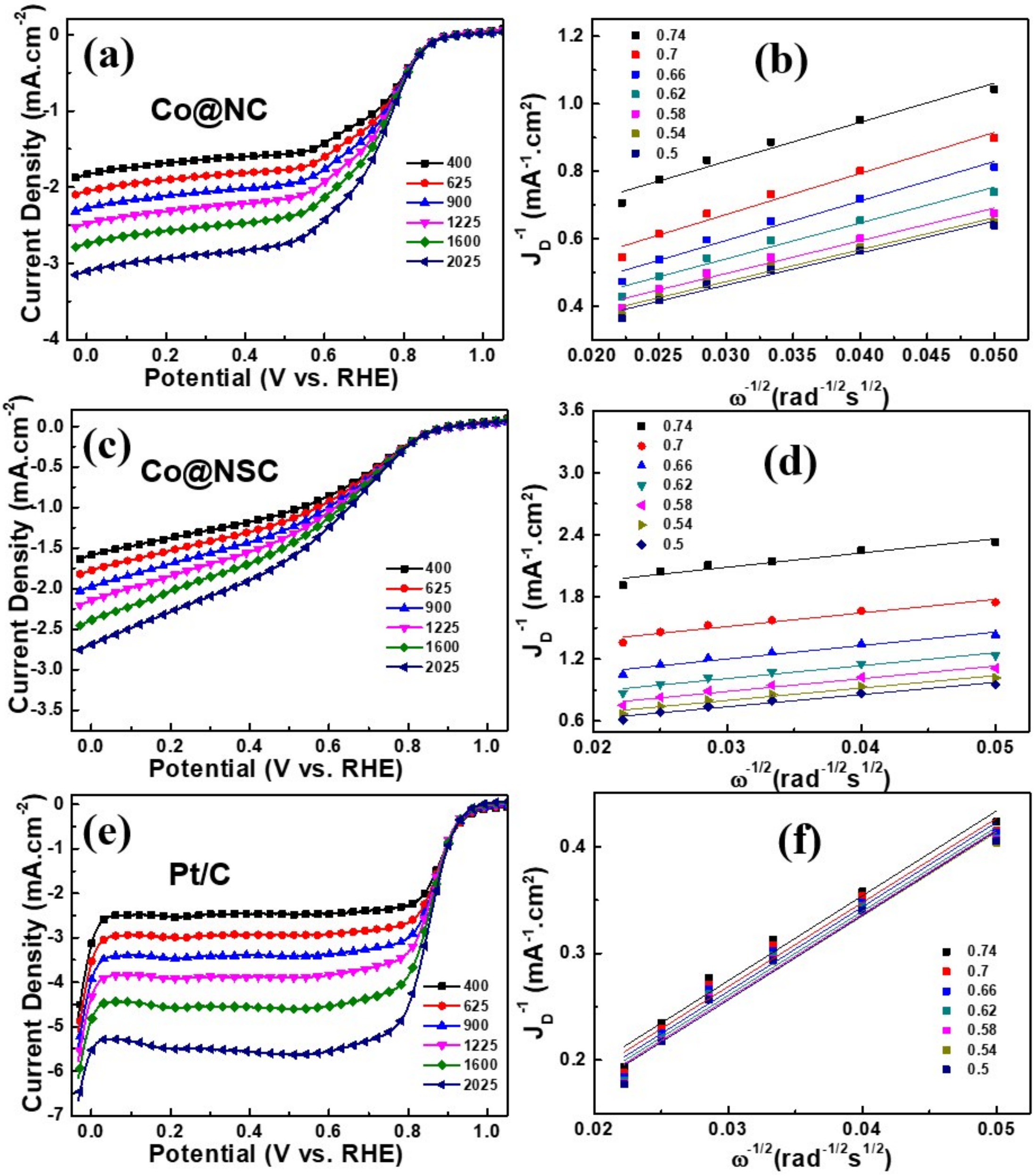

Figure S10. (a, c, e) RRDE curves and (b, d, f) K-L plots of Co@NC, Co@NSC and Pt/C in O_2-saturated 0.1 M KOH solution, respectively.

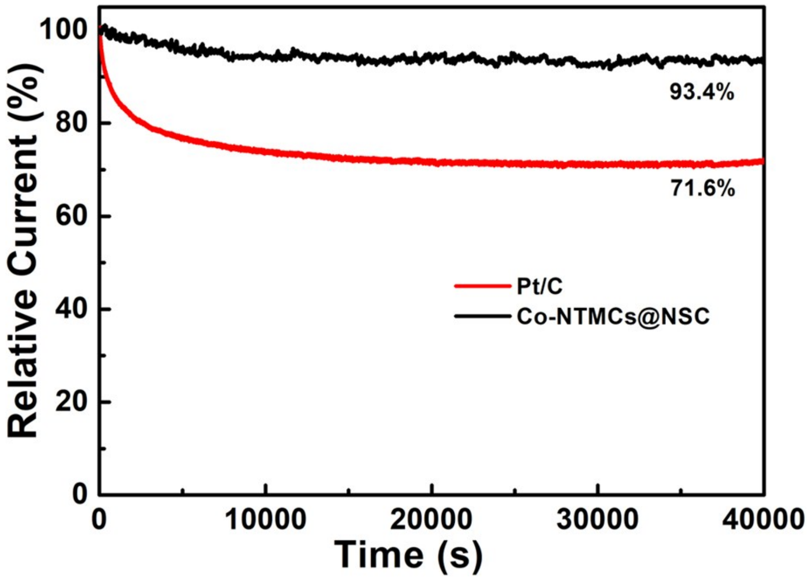

Figure S11. Chronoamperometric measurements of Co-NTMCs@NSC and Pt/C +0.50 V vs. RHE in an O_2-saturated 0.1 M KOH electrolyte at an electrode rotation rate of 900 rpm.

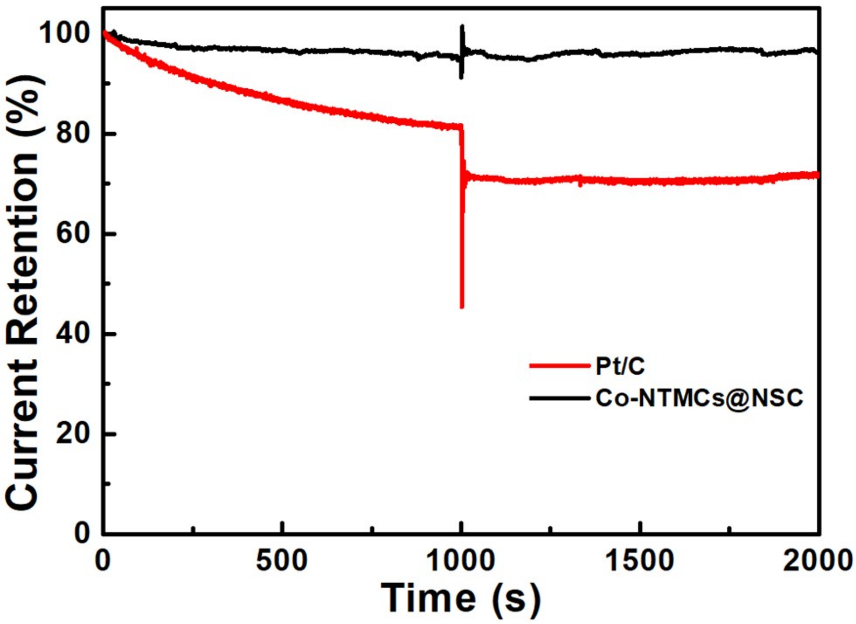

Figure S12. Chronoamperometric responses of Co-NTMCs@NSC and Pt/C in O_2-saturated 0.1 M KOH in the presence of 1 M methanol solution at +0.50 V vs. RHE.

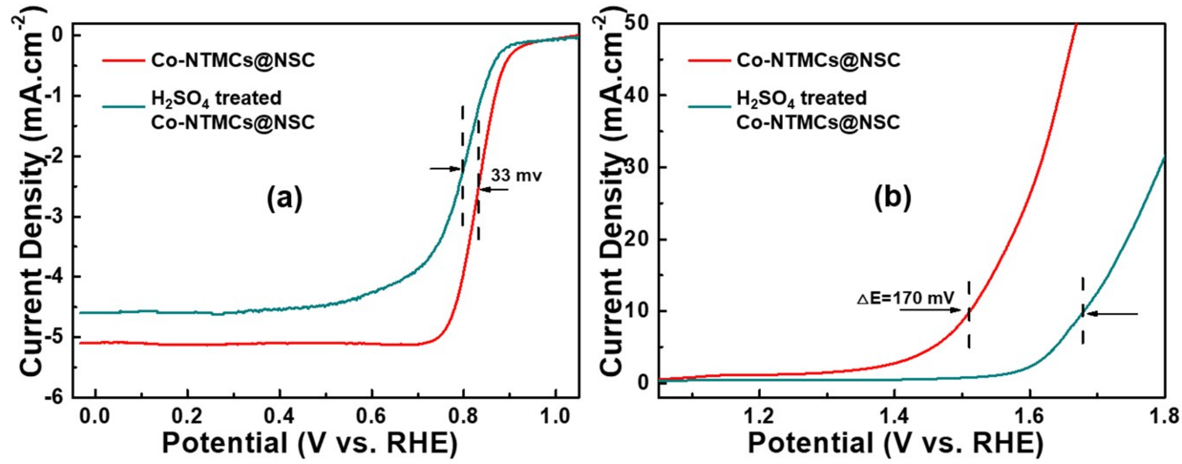

Figure S13. (a) LSV curves of Co-NTMCs@NSC for ORR and (b) LSV curves of Co-NTMCs@NSC for OER before and after etching treatment with 0.5 M H_2SO_4 at 80 ℃.

Table S1. The comparison on the key parameters of some leading transitional metal-based catalysts in ORR and OER electrocatalysis conducted in 0.1 M KOH electrolyte.

Catalysts	ORR half-wave potential (V vs RHE)	OER potential at 10 mA/cm2 (V vs RHE)	$\Delta E = E_{j=10} - E_{1/2}$	Ref.
N-GCNT/FeCo-3	0.92	1.73	0.81	Adv. Energy Mater. 2017, 7, 1602420
Cu@NCNT/Co_xO_y	0.82	1.6	0.78	Adv. Funct. Mater. 2017, 1705048
Co-N-CNTs	0.9	1.69	0.79	Adv. Funct. Mater. 2017, 1705048
$CoIn_2S_4$/S-rGO	0.82	1.6	0.78	Adv. Energy Mater. 2018, 1802263
N-GCNT/FeCo-3	0.92	1.73	0.81	Adv. Energy Mater. 2017, 7, 1602420
P, N Co-doped graphene	0.85	1.55	0.7	Energy Environ. Sci., 2017, 10, 1186-1195
ZIF-9_Fe3_Pyro	0.81	1.62	0.81	J Power Sources, 2019, 427, 299
Fe-N-C	0.84	1.6	0.76	J. Am. Chem. Soc. 138, 32, 10226-10231
Co@Co_3O_4/NC-1	0.8	1.65	0.85	Angew.Chem.Int. Ed. 2016, 55,4087–4091
Co@Co_3O_4/NC-2	0.74	1.64	0.9	Angew.Chem.Int. Ed. 2016, 55,4087–4091
CoS_x@PCN/rGO	0.78	1.57	0.79	Adv. Energy Mater. 2018, 8, 1701642
rGO/CB_2/Co-Bi	0.7	1.58	0.87	Adv. Energy Mater. 2018, 1801495
Pt/C+RuO_2	**0.85**	**1.59**	**0.74**	**This work**
Co-NTMCs@NSC	**0.83**	**1.59**	**0.76**	**This work**

Reference

[R1] Y. Niu, X. Huang, X, Wu, L. Zhao W. Hu and C. M. Li, One-pot synthesis of Co/N-doped mesoporous graphene with embedded Co/CoOx nanoparticles for efficient oxygen reduction reaction, Nanoscale, 2017, 9,10233–10239.